*Journal of Modern Optics*
Vol. 00, No. 00, DD Month 200x, 1–12

# *Enhanced recollision dynamics via the combination of antisymmetric wave functions and beyond-dipole effects*[*]

R. Fischer [†], M .Lein [‡†], C. H. Keitel[†]

[†]Max-Planck-Institut für Kernphysik, Saupfercheckweg 1, 69117 Heidelberg, Germany

[‡]Institut für Physik, Universität Kassel, Heinrich-Plett-Straße 40, 34132 Kassel, Germany

*(v1.0 released April 2006)*

The concept to enhance recollisions after laser-induced ionisation of antisymmetric molecular orbitals and of antisymmetric atomic wave functions is investigated. The underlying mechanism, first motivated by classical arguments, is based on partial compensation of the electron drift induced by antisymmetry and the drift induced by the laser magnetic field. The numerical solution of the time-dependent Schrödinger equation confirms our concept in terms of the increase of the harmonic signal for the first excited antisymmetric state of $H_2^+$, as an important example of a recollision-dependent process, but also reveals novel aspects of two-centre interference structures in high-harmonic spectra. Finally density contour plots illustrate the recollisions from antisymmetric orbitals and the virtues of employing ions rather than molecules.

## 1 Introduction

In the field of high-intensity laser-matter interactions the recollision dynamics of electrons ejected by a strong laser pulse is the basis of various strong-field phenomena like high-order harmonic generation (HHG) [1], nonsequential double ionisation [2] and above-threshold [3] ionisation. For instance, high-order harmonic generation in molecules is of particular interest in both theoretical and experimental studies at present. In recent investigations it has been shown that high-order harmonic radiation serves as a means to reconstruct molecular orbitals from HHG-spectra [4]. Whereas for both *atoms* and *molecules* a three-step mechanism is responsible for HHG [5], additional signatures in HHG-spectra of molecules are found which allow to draw conclusions about the separation of the nuclei and even about their vibrational motion [6]. Additionally, the anisotropy of molecular orbitals is reflected in the dependence of the corresponding HHG-spectra on the orientation of the orbital to the laser polarisation direction [7]. The underlying three-step process consists first in the ejection of an electron as an atom or a molecule is subject to a strong laser pulse. This is accomplished by electron tunneling through the potential barrier tilted by the laser field. In the second step the tunneled electron performs a quasi free oscillatory motion in the laser field. When the laser field changes its sign the electron wave packet is driven back to the nucleus. In the third step which represents the recollision event the wave packet recombines at the location of the nucleus into the initial state under emission of high-harmonic radiation. Considering this last step, it becomes plausible that the additional molecular degrees of freedom as vibration of the nuclei and the anisotropy of molecular orbitals may sensitively affect this recombination process. Therefore, signatures of molecular structure can be found in HHG-spectra. We would like to emphasize that the investigation of orientation-dependent characteristics in HHG-spectra and their relation to molecular symmetry opens up an interesting field of research [8]. This is particularly interesting in terms of the alignment techniques [9] which allow to bring a molecule in the desired orientation with regard to the polarisation direction of a strong laser field. Recently, it has been shown for an $H_2^+$ model ion that the peculiarities of the momentum distribution of antisymmetric molecular orbitals, which give rise to a lateral drift of electrons ejected by the laser field, can be employed to efficiently compensate for the electron drift induced by the

[*]dedicated to Prof. Sir Peter L. Knight FRS on the occasion of his 60th birthday
[†]Corresponding author. Email: keitel@mpi-hd.mpg.de

*Journal of Modern Optics*
ISSN 0950-0340 print/ISSN 1362-3044 online 
http://www.tandf.co.uk/journals
DOI: 10.1080/0950034YYxxxxxxxx

laser magnetic field of a very intense laser field [10]. As a result, there is an enhancement of recollisions. Moreover, HHG has turned out to provide a coherent light source, in which multiples of the irradiated laser frequency are gained [11] - even attaining the sub-Ångström regime [12]. This possibility to generate radiation of extreme short wavelengths has potential to investigate (bio)-chemical reactions with unprecedented resolution [13]. At present, high-harmonic radiation is employed as a tool to generate attosecond pulses [14]. With this it renders new fundamental pump-probe experiments possible.
However, the application of high-intensity laser pulses incurs the detrimental impact of the laser magnetic field drift [16] on the recollision dynamics. In view of the above mentioned important recollision-related effects a solution of this problem would be desirable. Several solutions have been proposed which consist in employing pre-accelerated particles [17], tailoring the applied laser pulse [18], using crossed laser fields [19] or choosing particular systems such as positronium [20]. As another solution mentioned above, it has very recently been shown how this drift can be compensated by means of antisymmetry of molecular orbitals. However, if one focuses on the generation of extreme short-wavelength harmonic radiation and if one therefore subjects molecules to very intense fields, one faces the problem that molecules whose outermost electrons are weakly bound are substantially ionised already during the turn-on phase of the laser pulse, i.e., the laser interaction with the molecules takes place in the over-the-barrier ionisation (OTBI) regime. Facing the problem of rapid ionisation it is advantageous to use antisymmetric *atomic* ions that withstand very intense laser fields. This allows for an efficient recollision dynamics and with this for the generation of extreme short-wavelength high-order harmonic radiation.

In this paper we apply the concept to harness the properties of antisymmetric wave functions in order to compensate for the electron drift induced by the laser magnetic field. This concept is applied to $H_2^+$ and to atomic ions. We consider excited eigenstates of hydrogen-like ions with antisymmetry with regard to a nodal line. These states have a similar shape as the antisymmetric wave function of the first electronically excited state of $H_2^+$ and they therefore possess the same properties of the momentum wave functions. We make use of them to compensate for the electron drift induced by the laser magnetic field. We obtain our results by numerical integration of the time-dependent Schrödinger equation on a 2D grid with and without employing the dipole approximation for very intense laser fields, respectively. Our model states are equivalent to real $2p$-atomic wave functions. The results for $H_2^+$ show the success of our method by the enhancement of high-order harmonic generation as an important recollision-related process. But in the wake of the interplay of antisymmetry and the drift induced by the laser magnetic field new effects concerning two-centre interference structures in HHG-spectra are found. The application of our method to antisymmetric atomic wave functions allows to see directly the enhanced recollision dynamics in contour plots of the electronic density.
Thus, the paper is organized as follows: In section 2 we explain in detail the underlying physical mechanism and the basic concept, i.e. the electron drift induced by the laser magnetic field, the properties of wave functions with mirror antisymmetry with respect to a nodal line and the combination of both in order to enhance recollisions and the harmonic signal. Section 3 is dedicated to the description of the numerical method employed. The results are presented for $H_2^+$ and then for hydrogen-like *atomic* ions in section 4. Concluding remarks are made in section 5.

## 2 Basic mechanisms and concept

For illustration, Fig. 1(a) shows the drift motion in laser propagation direction of a free electron subject to an intense laser pulse whose magnetic field component is responsible for this drift. The electron is initially at rest at the origin. If one is interested in the reduction of this drift in laser propagation direction one can choose appropriate initial conditions, i.e. with an initial velocity directed in the negative laser propagation direction. In Fig. 1(b) the initial velocity in laser propagation direction is -0.05 a. u. As a result, the drift in laser propagation direction can be reduced. Fig. 1(c) shows an over-compensation of the laser-induced drift due to an initial velocity of -0.53 a.u. which is the most probable initial velocity (momentum) in laser propagation direction for the lowest antisymmetric state of $H_2^+$ according to Fig. 2. This classical picture suggests a method to compensate for the drift induced by the laser magnetic field. In the following

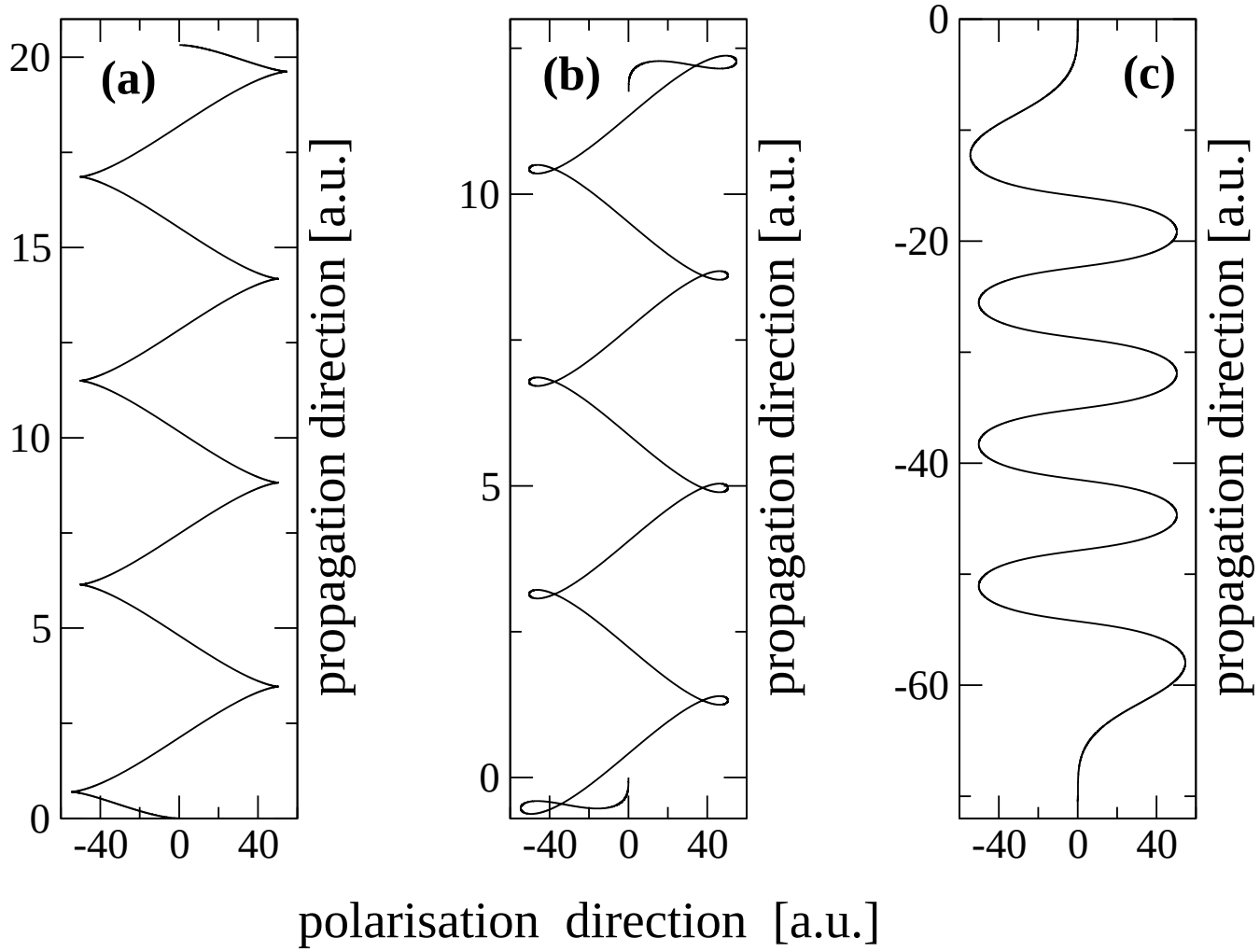


Figure 1. (a): Typical zig-zag motion of a classical electron subject to the trapezoidal laser pulse of an intensity $I = 1.4 \cdot 10^{17}\,\mathrm{W/cm^2}$ employed in the following quantum calculations. The electron has been initially at rest. The drift in laser propagation direction which is induced by the magnetic component of the laser field becomes more important for stronger fields.
(b): The drift in laser propagation direction is reduced by choosing appropriate initial conditions. In this figure the initial momentum in the laser propagation direction takes a value of -0.05 a. u. causing the electron to launch in the negative laser propagation direction. According to the momentum distribution due to antisymmetry in Fig. 2 there is a small but appreciable likelihood for this initial momentum.
(c): The drift in laser propagation direction is over-compensated by the choice of an initial momentum of -053 a.u., for which there is the largest likelihood according to Fig. 2.

quantum-mechanical considerations, however, the drift counteracting the laser-induced one is provided by antisymmetry. It is known for some time that this drift is also relevant for electrons ejected from an atom in a strong laser field. This process gives rise to a shift of the electron wave packet in the laser propagation direction. In accordance with the three-step model of HHG this implies for the generation of high-order harmonics that the overlap of recolliding wave packets with the initial wave function is reduced, which results in a decrease of the harmonic signal as a consequence of the laser magnetic field. Obviously, this detrimental influence of the laser magnetic field is not only relevant for HHG but also for other recollison-related effects like nonsequential double ionisation and high-order above threshold ionisation. As we point out in this article the magnetic field drift can be compensated by another drift which originates from the essence of antisymmetric wave functions. In this context, it becomes evident that the magnetically induced drift is able to increase recollisions and therefore can significantly support harmonic generation.

The properties of the momentum distribution of wave functions with mirror antisymmetry with respect to a nodal line are in the focus of this article. They are employed to affect the magnetically induced electron drift. The density of such a momentum wave function is shown in Fig. 2. This density illustrates

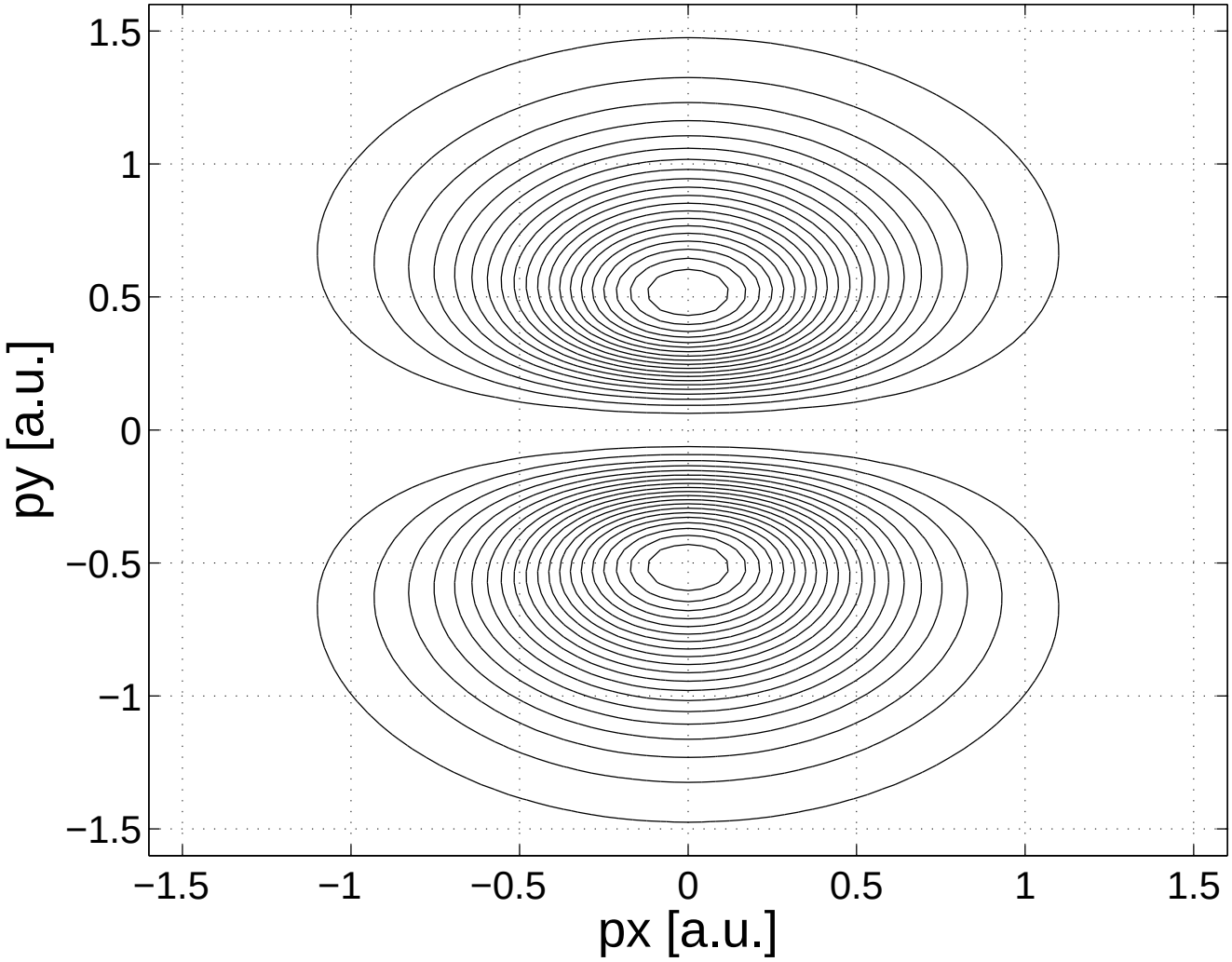


Figure 2. Density of the momentum wave function belonging to a wave function with mirror antisymmetry in position space (first excited state of $H_2^+$). It is obtained as the modulus square of the Fourier transform of the coordinate-space wave function. The anisotropy of this momentum distribution is responsible for the drift exhibited by electrons after field-assisted ejection: The figure illustrates clearly that the initial momentum of the electron is preferably directed in $y$-direction. The nodal line in this momentum distribution is responsible for the circumstance that there is no likelihood for momentum vectors directed strictly parallel to the $x$-axis. This means that no electrons are ejected strictly parallel to the $x$-axis during the interaction with the laser field if the field is applied along the $x$-axis.

the momentum distribution of the momenta $p_x$ and $p_y$ with regard to the $x$-axis and the $y$-axis, respectively. The corresponding 2D coordinate-space wave function lies in the $x$-$y$-plane with the nodal line being the $x = 0$-axis. Crucially, it is discernible that the probability for momentum vectors $(p_x, p_y)$ which are oriented strictly parallel to the $p_x$-axis, i.e., with no $p_y$-component, vanishes. This means that, if one considers such a wave function subject to a strong laser field along the $x$-axis as a reservoir of electrons, the ejected electrons have an initial drift perpendicular to the nodal line. This lateral drift incurred by the antisymmetry of the wave function affects sensitively all recollision-related effects, i.e., in particular HHG. If one considers a scenario in which an antisymmetric wave function is subject to an intense linearly polarised laser field with laser polarisation direction being the $x$-axis and the laser propagation direction being the $y$-axis, the recollision of ejected electrons and correspondingly HHG is suppressed in case of a nodal line aligned parallel to the polarisation direction. The tunneled electron is driven along the $x$-axis by the laser field. However, the electron has an initial drift in $y$-direction owing to the momentum distribution. Due to this drift the electron has been shifted in positive or negative $y$-direction, respectively, when the electron is accelerated back towards the nucleus again. From a classical point of view a recollision is precluded. Yet, also in a quantum picture, in which the wave packet spreading in $y$-direction has to be taken into account, an efficient recollision process is prevented. Keeping the $x$-axis as laser polarisation direction and

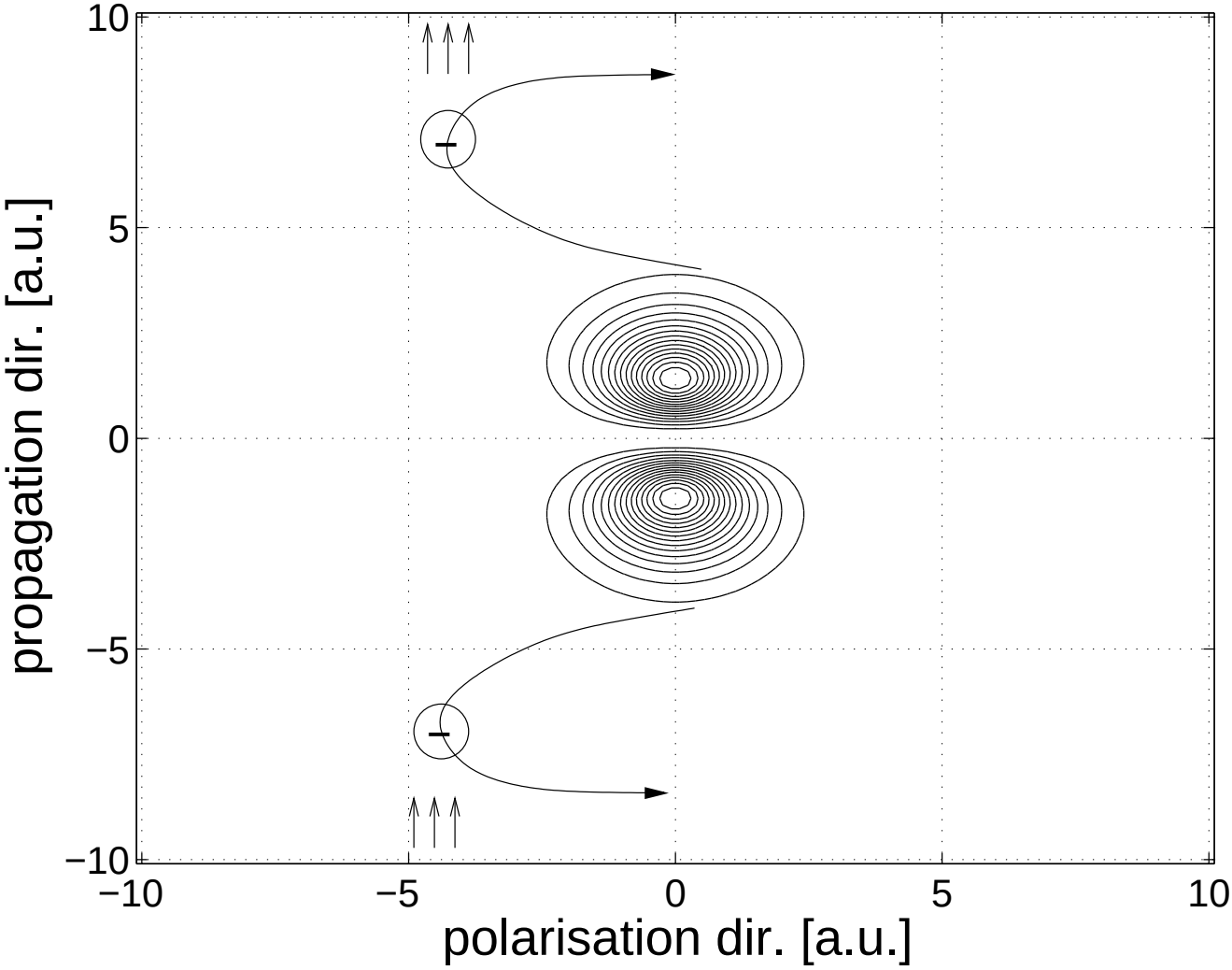


Figure 3. Antisymmetric wave function subject to a linearly polarised laser field. Shown is the initial antisymmetric state of 2D $H_2^+$ used in the following simulations. Ejected electrons travel preferably along the laser propagation direction. The magnetically induced electron drift helps to transfer the electron towards the molecular core, as indicated by the small arrows in the lower part of the figure.

the $y$-axis as laser propagation direction and rotating the antisymmetric initial wave function by 90°, so that the nodal line is finally parallel to the $y$-axis, results in an initial drift of ejected electrons along the laser polarisation direction. However, the laser electric field prevails in this direction. As a result, the drift induced by the antisymmetry of the wave function plays a minor role and HHG remains unaffected. The explanations above suggest that HHG is hampered the more parallel the nodal line is oriented to the laser polarisation direction. These considerations are only valid in the dipole approximation.

After having discussed the two basic effects, each taken for itself is detrimental to HHG, we introduce the concept to combine these two effects in order to increase recollisions and HHG. Fig. 3 shows an antisymmetric wave function subject to a strong laser field. The nodal line is parallel to the laser polarisation direction. Thus, the ejected electrons exhibit an initial lateral drift orthogonal to the nodal line, i.e., *along* the laser propagation direction. We employ this drift in order to compensate for the magnetically induced drift, which is indicated by the small arrows in the figure. Hence, this leads to an enhanced recollision probability and an increased harmonic signal. Note that in the lower part of the figure the electron is transferred *towards* the nucleus (nuclei) as a result of the magnetically induced drift, while this drift supports the drift induced by antisymmetry *away* from the nucleus (nuclei) in the upper part of the figure. However, our results demonstrate that, as a net effect, this constellation gives rise to enhanced recollisions and increased harmonic signals. If one rotates the initial wave function so that the nodal line is oriented in a certain angle to the laser polarisation direction the drift induced by antisymmetry can less success-

fully counteract the magnetically induced drift. In the case that the nodal line is orthogonal to the laser polarisation direction the drift caused by antisymmetry is parallel to the laser electric field. Thus, the magnetically induced drift hampers, as usual, the recollision process and HHG.

## 3 Numerical method

We solve the time-dependent Schrödinger equation for the first excited antisymmetric state of a 2D $H_2^+$ molecule and a hydrogen-like *atomic* ion subject to an intense short laser pulse of linear polarisation, respectively. The Hamiltonian which governs the electron dynamics reads in atomic units (a.u.):

$$H(x,y,t) = \frac{1}{2}\mathbf{p}^2 + \frac{1}{c}A_x(y,t)p_x + \frac{1}{2c^2}A_x(y,t)^2 + V_{ion}(x,y)\ . \tag{1}$$

Here $t$ denotes the time and $c$ the speed of light. The $x$-axis denotes the laser polarisation direction, whereas the $y$-axis represents the laser propagation axis. The operator $\mathbf{p} = (p_x, p_y, 0)$ represents the canonical momentum. $A_x(y,t)$ is the non-vanishing component of the vector potential $\mathbf{A} = (A_x(y,t), 0, 0)$ describing the laser pulse. The envelope of the sine laser pulse possesses a trapezoidal shape. In the case of $H_2^+$ the nuclei are clamped. Although the nuclear motion may give rise to a small effect on the HHG spectrum (see the first two references in [6]), we neglect it here in order to concentrate on beyond-dipole effects which are larger in our regime of interest. The term $V_{ion}(x,y)$ describes the interaction of the two nuclei with the electron and is described by a double-well soft-core potential:

$$V_{ion}(x,y) = -\sum_{k=1,2}\frac{1}{\sqrt{(x-x_k)^2 + (y-y_k)^2 + \epsilon}}\,, \tag{2}$$

where $(x_1, y_1)$ and $(x_2, y_2)$ are the positions of the nuclei. The positions are given by $x_{1,2} = \pm R/2\cos\Theta$ and $y_{1,2} = \pm R/2\sin\Theta$. The simulations are carried out for different fixed angles $\Theta$ between the molecular axis and the laser electric field. The nuclear separation $R$ is set at 2 a.u. The soft-core parameter $\epsilon$ has been determined to 0.58 in order to reproduce the electronic eigenenergy of -0.67 a.u. of the first excited electronic state of $H_2^+$. In the case of a hydrogen-like ion the term $V_{ion}(x,y)$ represents merely one soft-core potential:

$$V_{ion}(x,y) = -\frac{a}{\sqrt{1 + x^2 + y^2}} \tag{3}$$

The soft-core parameter $a$ has been chosen as 10.96 so that the first excited state of this potential possesses an eigenenergy of -6.1 a.u. for $N^{6+}$ which corresponds to the real value. The initial wave function has been obtained by a spectral method [21]. We employ the split-operator algorithm to solve the time-dependent Schrödinger equation with Hamiltonian (1) [22]. Short-time propagators $U(x,y,t)$ are successively applied to the initial wave function:

$$\Psi(x,y,t+\Delta t) \approx U(x,y,t)\Psi(x,y,t)$$

with

$$U(x,y,t) = e^{-iH(x,y,t)\Delta t}$$

The whole propagation is divided into small time steps $\Delta t$. The propagator $U(x,y,t)$ is split in the following manner:

$$U(x,y,t) = e^{-i\mathbf{p}^2\Delta t/4}\, e^{-iA_x(y,t)p_x\Delta t/c}\, e^{-i(A_x(y,t)^2/2c^2+V_{ion}(x,y))\Delta t}\, e^{-i\mathbf{p}^2\Delta t/4} \tag{4}$$

In order to apply the exponential operators in Eq. (4) a series of FFT-routines is performed on the wave function. By switching between position and momentum representation one can avoid differentiations [16]. The coherent part of the harmonic spectrum is computed as the windowed Fourier transform of the expectation value of the dipole acceleration in the laser polarisation direction [23]. All simulations have been accomplished with a grid spacing of 0.15 a.u. in each direction. Each propagation is performed with 2048 time steps per optical cycle. In order to prevent the electron wave function from reflections at the grid boundaries it is damped down to zero by means of a $cos^{\frac{1}{8}}$-mask function.

## 4 Results

In order to give evidence to our concept for the increase of recollisions and with this for the enhancement of HHG, we have carried out various simulations for different angles $\theta$ between the intermolecular axis of an $H_2^+$ model system (see Eq. (2)) and the laser polarisation direction. To study the impact of the drift induced by the laser magnetic field the simulations have been accomplished both in dipole approximation and beyond this approximation. According to our concept, we expect an increase in recollisions if the drift due to antisymmetry and the magnetically induced drift mutually counteract. The direction of the former depends on the orientation of the molecule, while the latter can be switched on or off in the simulation depending on whether the spatial dependence of the vector potential is taken into account or not, respectively. HHG is a process which directly depends on the efficiency of recollisions of electron wave packets returning to the nuclei. We consider the spectrum of harmonic radiation which is polarised along the laser polarisation direction. The intensity of the harmonic signal is directly correlated with the efficiency of the recollision-recombination process.

Figs. 4 shows the spectrum of an $H_2^+$ model ion subject to a sine laser pulse of a peak intensity of $7.9 \cdot 10^{16}\,\mathrm{W/cm^2}$. The trapezoidal envelope of the pulse comprises one cycle linear turn-on, three cycles of constant intensity and one cycle linear turn-off. The wavelength of the laser pulse is 248 nm, corresponding to a KrF-laser system. The solid line depicts the spectrum obtained in the dipole approximation, whereas the dashed line represents a spectrum calculated without having employed the dipole approximation. Fig. 4 demonstrates for $\theta = 90°$ a considerable enhancement of the harmonic signal up to four orders of magnitude as a result of the circumstance that in this constellation the drift due to antisymmetry counteracts the laser induced drift - in accordance with the concept presented. This is attributed to the compensation of both drifts. Evidently, the maximum enhancement of the harmonic signal is found for the $\theta = 90°$-orientation.

Fig. 5 sheds new light on two centre-interference effects in HHG-spectra which can be attributed to the presence of two nuclei. These effects have first been discovered and explained by the group of Knight ( see the first two references in [7]). Two-centre interference effects lead to typical minima and maxima in harmonic spectra. The location of these extrema is strongly dependent on the orientation of a diatomic molecule to the polarisation direction of a strong laser pulse. The occurrence of these structures are due to the interference of the recolliding wave packets with the initial state at the positions of the nuclei. This interference is strongly dependent on the orientation of the nuclei. Thus, different orientations of the molecule incur different locations of these extrema in the spectra. One obtains simple formulas predicting the positions of the extrema (see second reference in [7]). These formulas have been confirmed for the symmetric ground state wave function of $H_2^+$ in a situation where the dipole approximation has been justified. If we transfer these formulas to our situation of antisymmetric wave functions the minima $N_{min}$ would be sited at harmonic orders (see second reference in [7]):

$$N_{min} = \frac{2\pi^2 m^2}{R^2 \cos^2\theta\, \omega_L} \quad m = 0, 1, 2..., \tag{5}$$

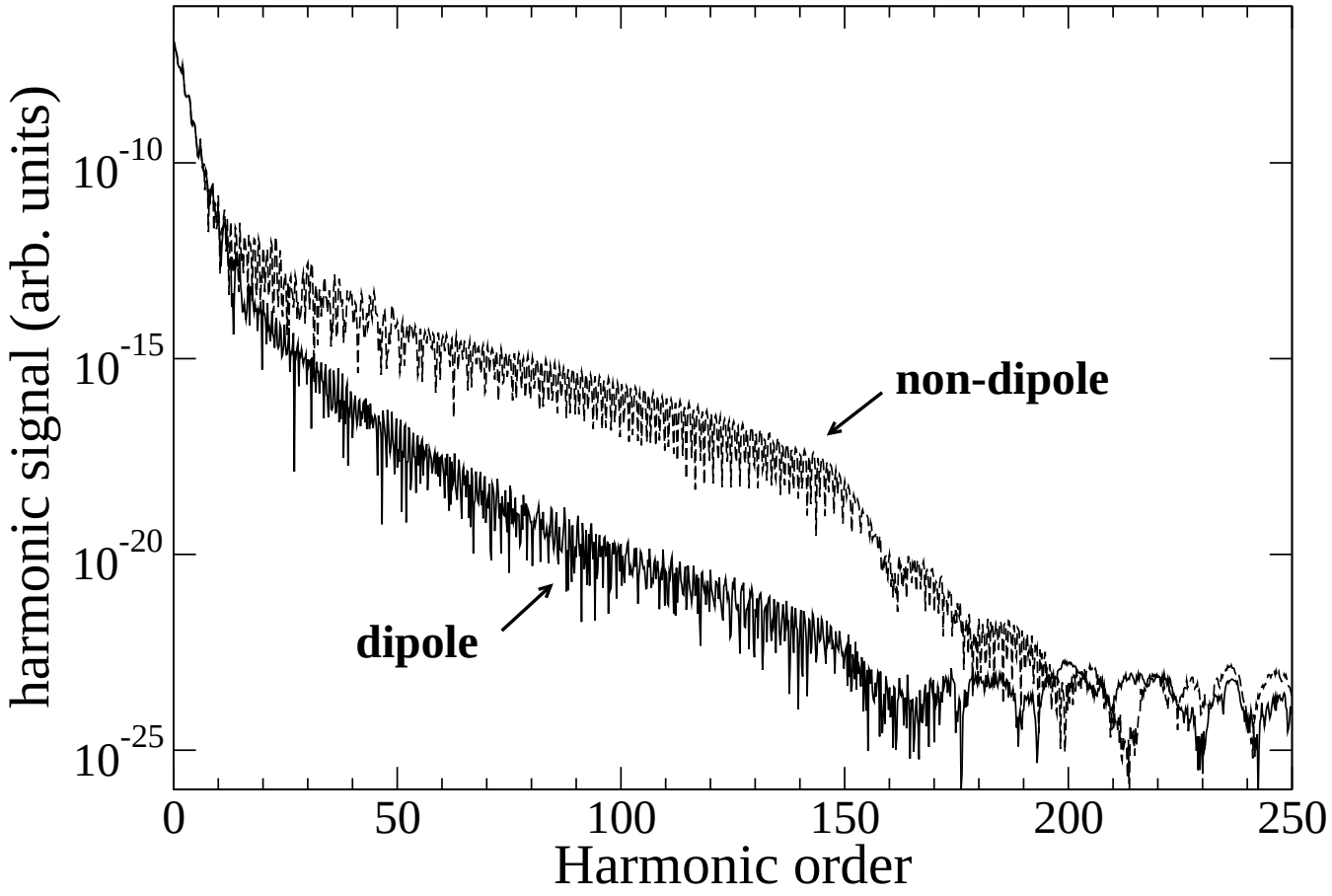


Figure 4. Harmonic spectrum of the first excited antisymmetric state of $H_2^+$ subject to a linearly polarised sine laser pulse of $7.9 \cdot 10^{16}\,\mathrm{W/cm^2}$. The trapezoidal shape of the pulse comprises one cycle linear turn-on, three cycles of constant intensity and one cycle linear turn-off. The laser wavelength is 248 nm. The solid line describes the spectrum obtained in the dipole approximation, whereas dashed one represents a calculation beyond this approximation. Note that the cut-off ($N_{max}$ =291) predicted by Eq. (6) is not attained owing to the rapid depletion of the initial wave function already in the turn-on phase of the pulse. For this $\theta = 90°$-orientation there is a dramatic enhancement in harmonic intensity due to the compensation of both drifts.

where $\omega_L$=0.18 a.u. denotes the laser frequency. Fig. 6 shows the positions of conspicuous interference minima for $\theta = 0°$ and $\theta = 50°$ for laser intensities of $I = 1.0 \cdot 10^{17}\,\mathrm{W/cm^2}$ and $I = 1.4 \cdot 10^{17}\,\mathrm{W/cm^2}$, respectively. The black lines represent spectra in the dipole approximation , while the red (grey) ones illustrate non-dipole spectra. For $m = 2$ Eq. (5) yields $N_{min} = 107$ for the $\theta = 0°$-alignment. This is in accordance with the spectra shown in Fig. 5(a),(c) for both the dipole and the non-dipole case, as indicated by the arrows. However, for angles $\theta$ different from 0° the positions of the minima in the spectra do not comply with Eq.(5) (For $\theta = 50°$: $N_{min} = 65$ for $m = 1$ or $N_{min} = 260$ for $m = 2$). Instead, for $\theta = 50°$ Fig. 5(b) yields a minimum at the 131st harmonic order in the dipole approximation or the 151st harmonic order in the non-dipole case for a laser intensity of $I = 1.0 \cdot 10^{17}\,\mathrm{W/cm^2}$, as indicated by arrows. For a higher laser intensity of $I = 1.4 \cdot 10^{17}\,\mathrm{W/cm^2}$ (Fig. 5(d)) the minimum is found at the 153rd harmonic order in the dipole case and at the 181st harmonic order in the non-dipole case.

Thus, we remark two new characteristics for these two-centre interference minima: First, we find clear signatures of non-dipole effects in two-centre interference structures. For $\theta \neq 0°$ we see a displacement of the minima towards higher harmonic orders in the non-dipole case. This might be attributed to the circumstance that the recolliding wave packets which are responsible for the interference minima gain additional kinetic energy by momentum transfer of the laser photons. For $\theta = 0°$ the displacement in the laser propagation direction of the recolliding wave packet does not seem to affect the interference but merely reduces the harmonic signal.

Second, for the first excited *antisymmetric* state of $H_2^+$ the locations of the minima do not correspond to the positions predicted by Eq.(5) for $\theta \neq 0°$. One reason for this might be that for antisymmetric initial states the ionisation dynamics is strongly dependent on the orientation, i.e. the shape and the

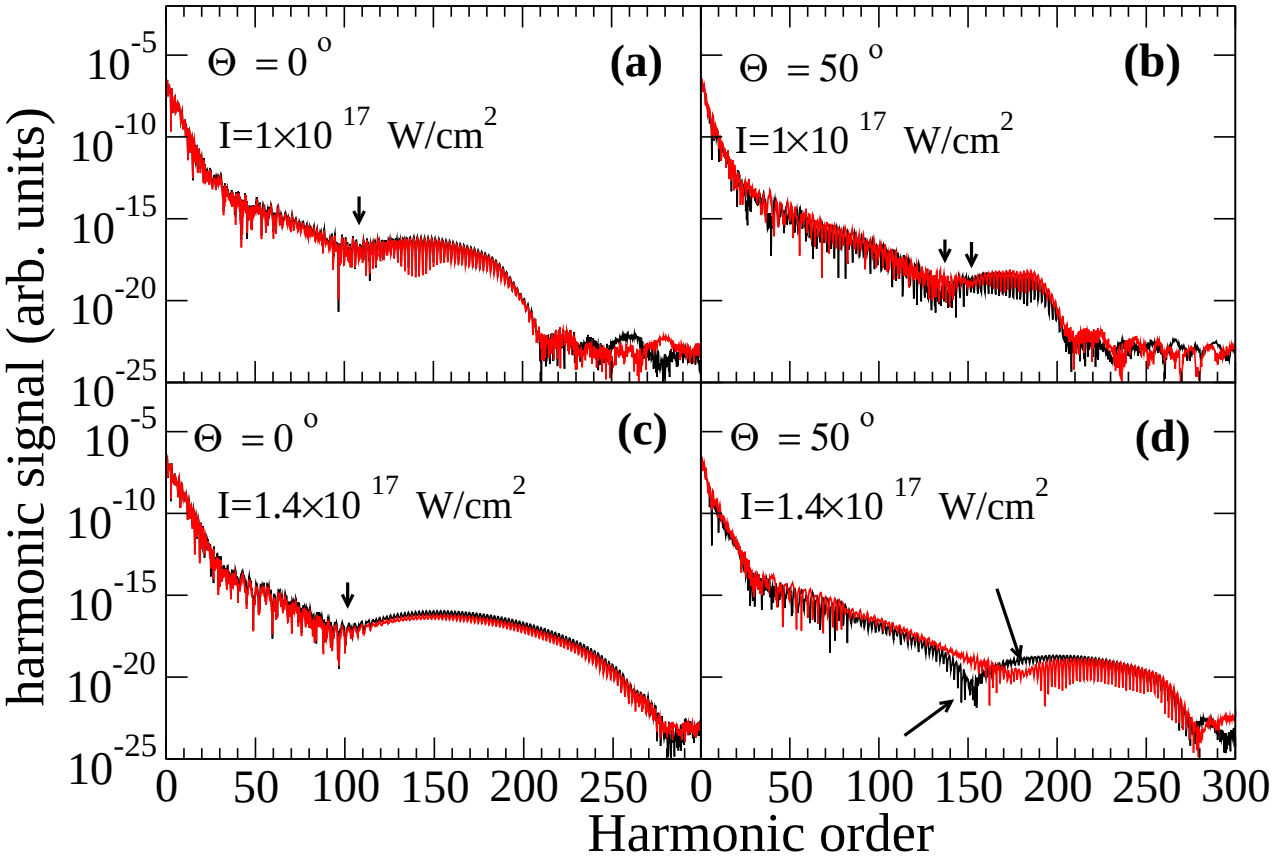


Figure 5. High-harmonic spectra for the antisymmetric first excited state of $H_2^+$. The black lines depict spectra obtained in the dipole approximation, while the red (grey) ones illustrate non-dipole results. The arrows indicate the positions of two-centre interference minima. For $\theta = 0°$ these minima lie in the vicinity of the 107th harmonic order which is predicted by Eq. (5), see parts (a),(c). Part (b) shows that for $\theta = 50°$ and an laser intensity of $I = 1.0 \cdot 10^{17}\,\mathrm{W/cm^2}$ the conspicuous minimum is located at the 135th harmonic order (dipole case) or at the 151st harmonic order (non-dipole case), respectively. For a higher laser intensity of $I = 1.4 \cdot 10^{17}\,\mathrm{W/cm^2}$ , see part (d), the minimum is found at the 153rd harmonic order (dipole case) or at the 181st harmonic order (non-dipole case), respectively. This shows the dependence of two-centre interference structures on the laser intensity for *antisymmetric* molecular orbitals. Furthermore, the drift induced by the laser magnetic field turns out to be responsible for a displacement of these interference structures towards higher harmonic orders in this high-intensity regime.

structure of the continuum wave packet is strongly dependent on how the electron is promoted into the continuum. In the succeeding recollision-recombination process the details of the recolliding wave packets might play a decisive role for the interference with the initial state. This is backed by our observation that the position of these minima is also dependent on the intensity of the laser pulse (Fig. 5(b),(d)). Further research should be dedicated to these two-centre interference effects for *antisymmetric* states. However, the dependence of the interference minima on the laser intensity suggests that an analytical description would be challenging.

We remark that for the highest laser intensity of $1.4 \cdot 10^{17}\,\mathrm{W/cm^2}$ in this article and a laser angular frequency $\omega_L$ of 0.18 a.u. the quiver velocity of a free electron, which is the relation of the laser electric field amplitude to the angular frequency, takes a value of 8 % of the speed of light. Therefore, higher-order relativistic effects, beyond the magnetic-field phenomena, can be safely neglected [16].

Furthermore, exposing fragile molecules with small binding energies, like $H_2^+$, to these high-intensity laser pulses employed in this article results in the circumstance that the maximum harmonic orders $N_{max}$

which are in principle possible cannot be achieved. These cut-off harmonic orders $N_{max}$ are given by [5]:

$$N_{max} = (I_P + 3.17\,U_P)/\omega_L \quad , \tag{6}$$

where $I_P$ denotes the ionisation potential of the molecule and $U_P$ represents the ponderomotive energy of the laser field. For the first (purely electronically) excited state of $H_2^+$ $I_P$ takes a value of 0.67. Hence, $N_{max}$=291, $N_{max}$=373 or $N_{max}$=515 for a laser intensity of $7.9 \cdot 10^{16}\,\mathrm{W/cm^2}$, $1.0 \cdot 10^{17}\,\mathrm{W/cm^2}$ or $1.4 \cdot 10^{17}\,\mathrm{W/cm^2}$, respectively. These cut-off harmonic orders are clearly not attained, as Fig. 4 and 5 show. This can be attributed to the rapid depletion of the initial state already during the turn-on phase of the pulse. Thus, the wave packets recolliding with the maximum possible kinetic energy of $3.17\,U_P$ cannot be ejected. As a result, the emission of radiation with a harmonic order $N_{max}$ according to Eq. (6) is suppressed. However, if one is interested in an efficient recollision dynamics and with this in the generation of extremely high harmonics and if one nevertheless intends to exploit the two drifts for mutual compensation, it is worthwhile investigating the laser-driven electron dynamics in highly charged hydrogen-like ions. The initial state in these *atomic* systems has to be antisymmetric with regard to a nodal line, i.e., the electron is initially in the first excited state which corresponds to 2p-orbitals in three dimensions. As pointed out in section 2 these wave functions exhibit the same drift properties due to antisymmetry as molecular orbitals. However, these *atomic* wave functions can withstand more intense laser fields because of higher binding energies.

For the illustration of the electron dynamics in $N^{6+}$ in the case of an orientation with the nodal line parallel to the laser polarisation direction , Fig. 6 shows snapshots of the logarithm of the electronic density during the interaction with the laser pulse. The snapshots are taken after one cycle ((a),(c)) and after 1.4 cycles ((b),(d)), respectively. Parts (a),(b) are obtained in the dipole approximation, while parts (c),(d) represent non-dipole results. In all four snapshots it is clearly visible that the major part of population remains at the position of the nucleus with the nodal line parallel to the laser polarisation direction ($x$-axis). This shows that the ion is able to withstand the strong laser pulse, i. e. only a minor part of the population is transferred into the continuum. Therefore, it becomes directly obvious that rapid initial ionisation is suppressed in the case of atomic ions. This clearly represents an advantage of antisymmetric atomic ions over fragile molecule. (Density plots in the molecular case are given in [10], where substantial ionisation occurs already in the turn-on phase of the laser pulse.) Fig. 6(a) illustrates the ejection of wave packets in the laser polarisation direction. It demonstrates clearly by its sickle-shaped density distribution the drift along the laser propagation direction ($y$-axis) owing to antisymmetry. Moreover, the symmetry of the density distribution with regard to the nodal line ($y$-axis) expresses the conservation of antisymmetry of the wave function (Fig. 6(a),(b)) in the dipole case. In contrast to this, the antisymmetry is broken beyond the dipole approximation; the density is displaced in the laser propagation direction (towards the positive $y$-axis), see Fig. 6(c),(d). Figs. 6(b)(d) show on the one hand new ejection of wave packets, going out left, as the laser field has changed its sign. On the other hand, even more interestingly, one can directly see the interplay of the drift due to antisymmetry and the drift induced by the laser magnetic field: The wide spread wave packets in parts (b),(d) represent wave packets which are accelerated back towards the core and which have been ejected in the laser cycle before. Comparing part (b) with (d), the distance of the wide spread wave packet to the $y = 0$-line in the lower part of Fig. 6(d) is smaller than the corresponding one in 6(b). This illustrates clearly the enhanced recollision dynamics of the returning wave packet with the initial state if one compares the density of Fig. 6(b) with the one of Fig. 6(d) in the vicinity of the origin. The fringes in the density distribution Fig.6(b),(d) suggest interference of recently ejected wave packets towards the left with the wide spread recolliding wave packet.
The enhanced recollision dynamics for antisymmetric atomic wave functions gives also rise to an increased emission of high-order harmonic radiation, where the realisation of the cut-off formula (6) and a substantially larger harmonic signal in comparison to molecular orbitals is possible in spite of the very high laser intensities [24].

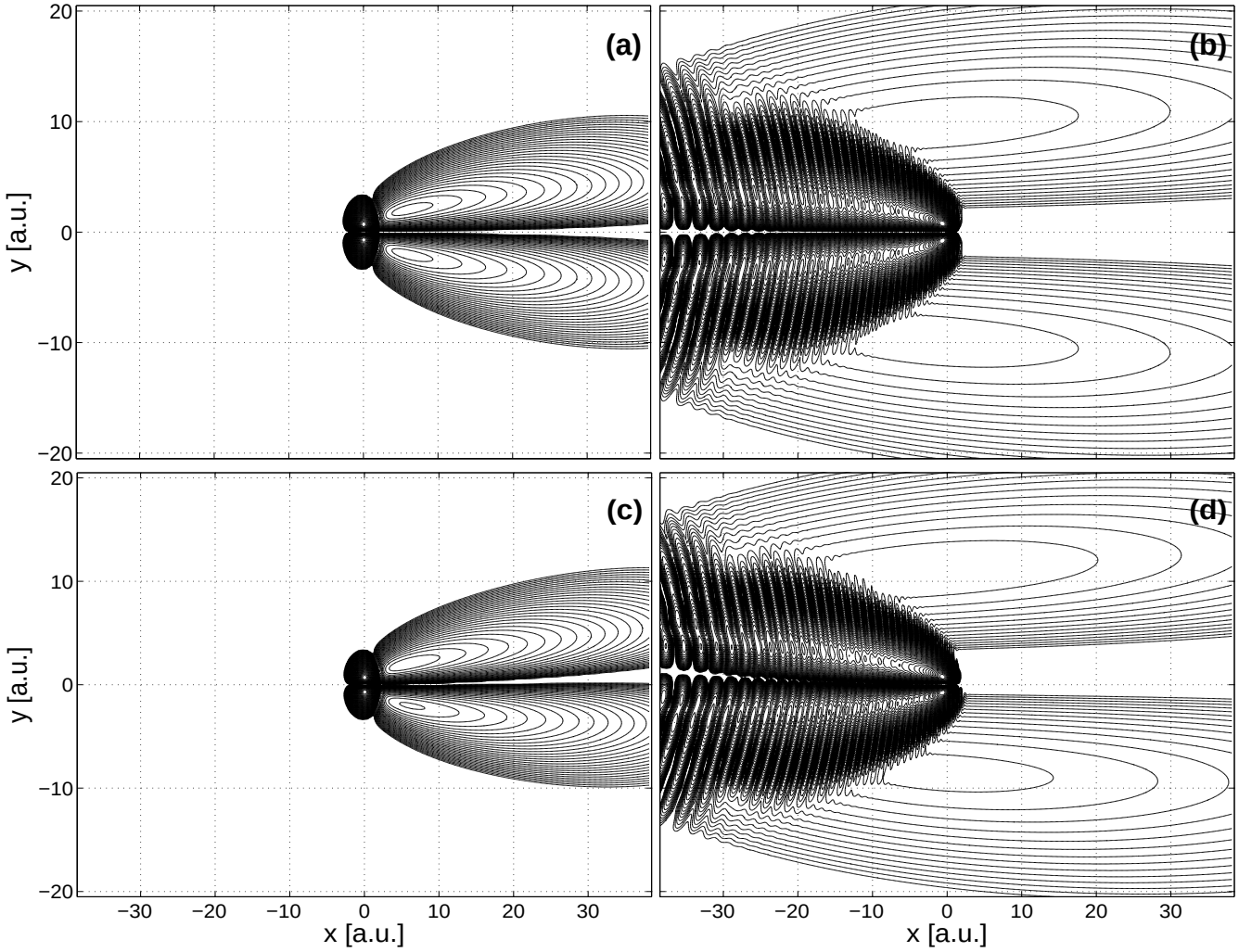


Figure 6. Snapshots of the logarithm of the electronic density during the laser pulse interaction after one cycle ((a),(c)) and 1.4 cycles ((b),(d)). Shown are plots with 60 contour lines, only values of a density above $10^{-12}$ are taken into account. Parts (a),(b) depict dipole results, whereas parts (c), (d) illustrate the non-dipole case. The sickle-shaped density distribution of outgoing wave packets towards the right side in parts (a), (c) and towards the left in part (b), (d) of the figure show directly the lateral drift due to antisymmetry. In parts (b), (d) the wide spread wave packet recollides with the wave packets in the vicinity of the nucleus. Comparing (b) with (d), the enhanced recollision dynamics due to the interplay of the drift due to antisymmetry and the magnetically induced drift in laser propagation direction ($y$-axis) is clearly visible; note the distance between the wide spread recolliding wave packet and the $y = 0$-line.

## 5 Conclusion

We have investigated two basic effects for laser-driven ionisation of an antisymmetric wave function (molecule and atom). On the one hand, one has to take the drift into account which is induced by the antisymmetry of the wave function. This drift is responsible for a strong orientation dependence of recollision-related effects like HHG. On the other hand, the drift in laser propagation direction which is induced by the laser magnetic field becomes crucial for very intense laser fields. Each effect taken for itself is detrimental to the recollision dynamics and with this to HHG. We have given evidence by the numerical integration of the time-dependent Schrödinger equation that the combination of both effects is able to give rise to an enhancement of recollisions and HHG. In this context we have pointed out new aspects for two-centre interference structures in HHG-spectra of antisymmetric molecular orbitals, in particular, non-dipole effects are shown to become relevant for two-centre interference in the high-intensity regime. Moreover, we have directly illustrated the enhanced recollision dynamics by means of contour plots of the electronic density in the case of antisymmetric atomic wave functions.

## References


[1] T. Kanai, S. Minemoto, and H. Sakai, Nature **435**, 470 (2005); H. Niikura *et al.*, Nature **417**, 917 (2002); A. D. Bandrauk and H. Z. Lu, Phys. Rev. A **73**, 013412 (2006).

[2] R. Dörner, Th. Weber, M. Weckenbrock, A. Staudte, M. Hattass, R. Moshammer, J. Ullrich, and H. Schmidt-Böcking, Adv. At., Mol., Opt. Phys. **48**, 1 (2002); P. J. Ho, R. Panfili, S. L. Haan, and J. H. Eberly, Phys. Rev. Lett. **94**, 093002 (2005); J. Prager and C. H. Keitel, J. Phys. B **35**, L167 (2002).

[3] D. B. Milošević, G. G. Paulus, D. Bauer, and W. Becker, J. Phys. B **39**, R203 (2006); F. Lindner *et al.*, Phys. Rev. Lett. **95**, 040401 (2005); G. G. Paulus, F. Zacher, H. Walther, A. Lohr, W. Becker, and M. Kleber, Phys. Rev. Lett. **80**, 484 (1998).

[4] J. Itatani *et al.*, Nature **432**, 867 (2004).

[5] P. B. Corkum, Phys. Rev. Lett. **71**, 1994 (1993); M. Lewenstein, Ph. Balcou, M. Yu. Ivanov, Anne L'Huillier, and P. B. Corkum, Phys. Rev. A **49**, 2117 (1994).

[6] W. Qu, Z. Chen, Z. Xu, and C. H. Keitel, Phys. Rev. A **65**, 013402 (2001); M. Lein, Phys. Rev. Lett. **94**, 053004 (2005); C. C. Chirila and M. Lein, J. Phys. B **39**, S437 (2006); S. Baker *et al.*, Science **312**, 424 (2006).

[7] M. Lein, N. Hay, R. Velotta, J.P. Marangos, and P.L. Knight, Phys. Rev. Lett. **88**, 183903 (2002); M. Lein, N. Hay, R. Velotta, J.P. Marangos, and P.L. Knight, Phys. Rev. A **66**, 023805 (2002); M. Lein, J.P. Marangos, and P.L. Knight, Phys. Rev. A **66**, 051404(R) (2002); D. G. Lappas and J. P. Marangos, J. Phys. B **33**, 4679 (2000); R. Velotta, N. Hay, M. B. Mason, M. Castillejo, and J. P. Marangos *et al.*, Phys. Rev. Lett. **87**, 183901 (2001); C. Vozzi *et al.*, Phys. Rev. Lett. **95**, 153902 (2005).

[8] X. X. Zhou, X. M. Tong, Z. X. Zhao, and C. D. Lin, Phys. Rev. A **72**, 033412 (2005); X. X. Zhou, X. M. Tong, Z. X. Zhao, and C. D. Lin, *ibid.* **71**, 061801(R) (2005); B. Shan, S. Ghimire, and Z. Chang, *ibid.* **69**, 021404(R) (2004); T. K. Kjeldsen, C. Z. Bisgaard, L. B. Madsen, and H. Stapelfeldt, Phys. Rev. A **68**, 063407 (2003); M. Lein, J. Phys. B **36**, L155 (2003).

[9] H. Stapelfeldt and T. Seideman, Rev. Mod. Phys. **75**, 543 (2003); F. Rosca-Pruna and M. J. J. Vrakking, J. Chem. Phys. **116**, 6567 (2002); J. J. Larsen, K. Hald, N. Bjerre, H. Stapelfeldt, and T. Seideman *et al.*, Phys. Rev. Lett. **85**, 2470 (2000).

[10] R. Fischer, M. Lein, and C. H. Keitel, Phys. Rev. Lett. **97**, 143901 (2006).

[11] Y. I. Salamin, S. X. Hu, K. Z. Hatsagortsyan, and C. H. Keitel, Phys. Rep. **427**, 41 (2006); D. B. Milošević and F. Ehlotzky, Adv. At., Mol., Opt. Phys. **49**, 373 (2003); W. Becker, F. Grasbon, R. Kopold, D. B. Milošević, G. G. Paulus, and H. Walther , Adv. At., Mol., Opt. Phys. **48**, 35 (2002).

[12] C. H. Keitel and S. X. Hu, Apl. Phys. Lett. **88**, 541 (2002).

[13] J. C. Solem and G. C. Baldwin, Science **218**, 229 (1982); M. H. Vos and J.-L. Martin, Annu. Rev. Biophys. Biomol. Struct., **21**, 199 (1992); K. Boyer, J. C. Solem, J. W. Longworth, A. B. Borisov, and C. K. Rhodes, Nat. Med. (N. Y.) **2**, 939 (1996); C. Rose-Petruck *et al.*, Nature (London) **398**, 310 (1999).

[14] M. Drescher, M. Hentschel, R. Kienberger, G. Tempea, C. Spielmann, G. A. Reider, P. B. Corkum, and F. Krausz, Science **291**, 1923 (2001); M. Hentschel *et al.*, Nature **414**, 509 (2001); R. López-Martens *et al.*, Phys. Rev. Lett. **94**, 033001 (2005).

[15] S. X. Hu and C. H. Keitel, Europhys. Lett. **47**, 318 (1999); N. J. Kylstra, R. M. Potvliege, and C. J. Joachain, J. Phys. B **34**, L55 (2001).

[16] N. J. Kylstra, R. A. Worthington, A. Patel, P. L. Knight, J. R. Vazquez de Aldana, and L. Roso, Phys. Rev. Lett. **85**, 1835 (2000); S. X. Hu and C. H. Keitel, Phys. Rev. A **63**, 053402 (2001).

[17] G. R. Mocken and C. H. Keitel, J. Phys. B **37**, L275 (2004); C. C. Chirila, C. J. Joachain, N. J. Kylstra, and R. M. Potvliege, Phys. Rev. Lett. **93**, 243603 (2004).

[18] M. Klaiber, K. Z. Hatsagortsyan, and C. H. Keitel, Phys. Rev. A **74**, 051803(R) (2006).

[19] N. Milosevic, P. B. Corkum, and T. Brabec, Phys. Rev. Lett. **92**, 013002 (2004); H. K. Avetissian, A. K. Avetissian, G. F. Mkrtchian, and K. V. Sedrakian, Phys. Rev. E **66**, 016502 (2002).

[20] B. Henrich, K. Z. Hatsagortsyan, and C. H. Keitel, Phys. Rev. Lett. **93**, 013601 (2004); K. Z. Hatsagortsyan, C. Müller, and C. H. Keitel, Europhys. Lett. **76**, 29 (2006).

[21] M. D. Feit, J. A. Fleck, Jr., and A. Steiger, J. Comput. Phys. **47**, 412 (1982).

[22] J. Fleck, J. Morris, and M. Feit, Appl. Phys. **10**, 129 (1976); A D Bandrauk and H. Shen, J. Phys. A **27** 7147 (1994).

[23] K. Burnett, V. C. Reed, J. Cooper, and P. L. Knight, Phys. Rev. A **45**, 3347 (1992); T.-F. Jiang and S.-I. Chu, Phys. Rev. A **46**, 7322 (1992).

[24] R. Fischer, M. Lein, and C. H. Keitel, submitted.